

General Disclaimer

One or more of the Following Statements may affect this Document

- This document has been reproduced from the best copy furnished by the organizational source. It is being released in the interest of making available as much information as possible.
- This document may contain data, which exceeds the sheet parameters. It was furnished in this condition by the organizational source and is the best copy available.
- This document may contain tone-on-tone or color graphs, charts and/or pictures, which have been reproduced in black and white.
- This document is paginated as submitted by the original source.
- Portions of this document are not fully legible due to the historical nature of some of the material. However, it is the best reproduction available from the original submission.

**NASA TECHNICAL
MEMORANDUM**

NASA TM X-52645

NASA TM X-52645



**PRELIMINARY PERFORMANCE OF A 1200 HERTZ ALTERNATOR,
VOLTAGE REGULATOR, AND ELECTRONIC SPEED CONTROL
OPERATING IN A BRAYTON CYCLE POWER SYSTEM**

by Sheldon J. Meyer and Robert C. Evans
Lewis Research Center
Cleveland, Ohio
August 1969

FACILITY FORM 602	N69-34673	
	(ACCESSION NUMBER)	(THRU)
	27	1
	(PAGES)	(CODE)
	TMX-52645	09
	(NASA CR OR TMX OR AD NUMBER)	(CATEGORY)

This information is being published in preliminary form in order to expedite its early release.

**PRELIMINARY PERFORMANCE OF A 1200 HERTZ ALTERNATOR,
VOLTAGE REGULATOR, AND ELECTRONIC SPEED CONTROL
OPERATING IN A BRAYTON CYCLE POWER SYSTEM**

by Sheldon J. Meyer and Robert C. Evans

**Lewis Research Center
Cleveland, Ohio**

NATIONAL AERONAUTICS AND SPACE ADMINISTRATION

PRELIMINARY PERFORMANCE OF A 1200 HERTZ ALTERNATOR, VOLTAGE REGULATOR,
AND ELECTRONIC SPEED CONTROL OPERATING IN A BRAYTON
CYCLE POWER SYSTEM

by Sheldon J. Meyer and Robert C. Evans

Lewis Research Center

ABSTRACT

A single shaft turbine-compressor-alternator with electronic voltage and speed control was tested at approximately design turbine inlet temperature and speed with constant power output levels of 4.30, 5.02, and 6.08 kW. The purpose of this test was to check out the integrity of the design and the electrical component performance when operating in a Brayton cycle power generating system. All electrical components performed within design specifications although some aberrations were noted. The speed control introduced phase load unbalance. Load fluctuations were observed as each unit of the speed control began to apply load to the alternator. The fluctuations were small and did not result in changes of machine speed. The alternator armature windings operated with higher temperatures at 6 kW load than predicted. These temperatures are however within the design operating rating for the insulation on the windings.

PRELIMINARY PERFORMANCE OF A 1200 HERTZ ALTERNATOR, VOLTAGE REGULATOR,
AND ELECTRONIC SPEED CONTROL OPERATING IN A BRAYTON
CYCLE POWER SYSTEM

by Sheldon J. Meyer and Robert C. Evans

Lewis Research Center

SUMMARY

A single shaft turbine-compressor-alternator with electronic voltage and speed control was operated in a laboratory Brayton cycle power system. The purpose of the test was to verify the integrity of the system when operating at approximately design turbine inlet temperature and speed, and with constant loads on the alternator of 4.30, 5.02, and 6.08 kW. This report presents the results obtained from testing the alternator, voltage regulator, and electronic speed control at the three system load levels.

The electronic speed control maintained speed within the specified ± 1 percent. It changed the three phase load balance, however, for each system load level. Load fluctuations were observed at power levels corresponding to the frequency at which each speed control unit began to apply load. These fluctuations were small and did not result in any speed fluctuations. The mode of operation of the shunt field regulator was affected by line voltage distortion produced by the speed control, but voltage was regulated within the design specification of ± 1 percent. The alternator armature windings operated at higher temperatures than predicted.

INTRODUCTION

The Lewis Research Center is currently engaged in a technology program to develop components for Brayton Cycle Space Power Systems (ref. 1). As part of this program, a single shaft turbine-compressor-alternator unit with an electronic speed and voltage control system was procured under contract from the AiResearch Manufacturing Co. of Arizona for evaluation at Lewis.

The turbine-compressor-alternator unit which comprises the rotating component of the Brayton cycle power system is called the Brayton Rotating Unit or BRU. The BRU was designed to operate on self acting gas bearings at a speed of 36 000 rpm. The working fluid is a mixture of helium and xenon with a molecular weight of 83.8. The alternator is designed for 10.7 kW output at power factors ranging from 0.75 lagging to unity at 120/208 volts, three phase, 1200 hertz.

The first hot testing accomplished with the BRU was done at approximately design temperature for the purpose of checking out integrity of design and component performance and to gain assurance that there were no short term problems in operating with gas bearings (ref. 2). During these tests, the alternator was operated at steady state power output levels of 4 to 6 kW for the purpose of observing electrical component operating characteristics and interactions when operating in a power generating system.

This report presents the results obtained from preliminary tests of the BRU alternator, and Laboratory models of the voltage regulator-exciter and electronic speed control operated at three system power levels. Also included in this report are descriptions of the apparatus and test procedure.

SYMBOLS

A	true root mean square current indicator
E_R	d.c. reference voltage
e_B	instantaneous level of half wave three phase rectified signal obtained from the alternator output voltage
OSC	oscilloscope
T_C	transistor switch time closed interval line to neutral voltage
V	true root mean square voltage indicator
W	phase power indicator
W_T	total three phase power indicator

BRU DESCRIPTION

A photograph and schematic of the BRU are shown in figures 1 and 2. The turbine and the compressor are mounted on the ends of a common shaft with the alternator, the two journal bearings, and the thrust bearings located in between. Table I summarizes the design operating conditions for the turbine, compressor and gas bearings when operating at the 10.7 kW electrical load condition.

The design specifications for the BRU alternator are presented in table II. The alternator is an oil cooled brushless, solid-rotor, four pole, modified Lundell unit (ref. 3). Figure 3 gives a sectional view of the alternator showing details of the alternator construction. The rotor consists of two separate magnetic sections made of SAE 4340

with two north poles on one and two south poles on the other. These sections are brazed to a nonmagnetic separator made of Inconel 718. This rotor pole arrangement is shown in reference 4.

The alternator utilizes two independent fields. The shunt field is supplied by the voltage regulator to maintain the output voltage at the rated level. The series field is supplied by the series field static exciter using line current transformers. Its excitation level is proportional to the alternator three phase line currents. Under three phase fault conditions, this field would supply the excitation necessary to maintain short circuit current for the time interval needed for circuit protective devices to operate. Also, use of this exciter reduces the power requirements placed on the voltage regulator by supplying part of the field excitation required by the alternator under load.

Two separate helical channels are machined into the alternator outer frame assembly for cooling the field and armature windings. Each passage can be independently supplied with coolant. Only one channel required for alternator cooling. The second was added for increased system reliability.

VOLTAGE REGULATOR

The design electrical specifications for the voltage regulator-exciter are included in table II. A block diagram of the shunt field regulator portion of the voltage regulator (VR) is presented in figure 4. This regulator incorporates an unregulated power supply whose source of power is the three phase alternator output, a current limiting circuit, a regulated logic power supply, a transistorized switching circuit, a line voltage sensing circuit and a voltage comparison circuit (ref. 5). The comparison circuit has as its input a unidirectional signal proportional to the alternator output voltage and a constant reference voltage derived using a zener diode. The voltage comparison circuit output keys the transistor switch.

When the transistor switch closes, the total d.c. supply voltage is applied to the shunt field winding. The duration of closure is affected by the comparison circuit voltage output. The duty cycle of this switch determines the average value of the VR portion of the field current. This operation can be shown by using a graphical representation (fig. 5) showing the signals appearing in the comparison circuit in the VR. Attention must be given to the alternator line to neutral voltage waveforms, especially in regards to differences in peak values and to distortions occurring near the peaks. The output transistor switch operation is determined by the relationship between E_R , the d.c. reference voltage and E_B , the instantaneous level of the half wave, three phase rectified signal obtained from the alternator output voltage. The switch is open for $E_B > E_R$ and closed for

$e_B < E_R$. Distortion of individual phase ripple voltage wave shapes effects the time interval where $e_B < E_R$ as does differences in ripple peak magnitudes. If the ripple pattern is uniform, the VR output voltage would appear as pulses whose frequency is three times alternator line frequency.

The VR has a current limit circuit which holds shunt field current levels to within component ratings when the alternator output is below approximately 115 volts line-to-neutral (i.e., during BRU start-up). This overrides the transistor switch control normally provided by the voltage comparison circuit.

ELECTRONIC SPEED CONTROL

BRU speed control is obtained by automatically increasing a three phase electrical load in proportion to frequency error above a 1200 hertz reference point. As frequency increases, more load is applied by increasing the voltage across a constant value of resistance which acts as a three phase parasitic load resistor. This increase in voltage is performed by a 3 unit speed control which uses silicon controlled rectifiers (SCR's). The SCR's are controlled by a phase shift control circuit and their conduction point in the voltage cycle is determined by a signal proportional to the frequency error. Table II also includes design specifications for this unit.

The first unit of the speed control is adjusted to apply 6 kW of parasitic load for the first 1.2 percent of frequency error. The second adds an additional 6 kW for the error range of 1.2 to 2.4 percent as does the third for an error range of 2.4 to 3.6 percent. Each control unit consists of a frequency converter, magnetic amplifiers, three phase firing circuit and SCR output stages (see fig. 6 for block diagram) and senses frequency from a different alternator output phase. Each speed control unit has two variable adjustments. One sets the frequency at which it will begin to apply load. The range frequency error over which the units respond was adjusted to overlap. This could result in the second unit, for example, conducting before maximum conduction angles are reached on the first. The second adjustment effects the units response (slope of load applied versus frequency error curve).

APPARATUS

A schematic of the test loop is shown in figure 7. Starting at the compressor inlet, the gas flows through the compressor where its pressure is raised to the desired level. Next the gas flows through the heater where it is heated to the design temperature level. From the heater it flows through the turbine where power is extracted and on through the cooler where the excess heat is removed. The gas then flows to the compressor to begin the cycle again.

The lines to the gas bearings are for external pressurization during start-up and shutdown to prevent rubbing. At design speed the bearings are made completely self-acting by the removal of external pressurization. The compressor by-pass line is for emergency loop shutdown and manual speed control.

Figure 8 shows a block diagram of the Brayton electrical power and speed control system. Also shown is the location of instrumentation used to measure electrical system performance. The system load was not used during these tests.

PROCEDURE

Preliminary tests were conducted on the BRU to determine the effects of design turbine inlet temperature and speed on the performance of the gas bearings and to observe operation characteristics of electrical components in a Brayton cycle power generating system. During the tests, the alternator load did not exceed 6 kW.

The test procedure is described as follows. The speed of the BRU was brought up to approximately 35 000 rpm using the manually controlled valve in the compressor by-pass line. At this speed the VRE contactor was closed energizing the shunt field of the alternator. This raised the alternator output voltage from approximately 30 volts, (generated because of residual magnetic field intensity), to the design value of 120 volts. The contactor for the speed control-parasitic load was then closed. BRU speed was slowly increased by closing the manual compressor by-pass valve. At approximately 36 060 rpm (1202 Hz), the first unit of the speed controller began to apply load to the alternator. The speed control automatically increased the load as the turbine output was increased. The turbine inlet temperature was set at approximately 1960° R (1089 K) (100° below design) and the mass flow rate varied to give the required alternator output power. Design temperature was not achieved because of thermal limitations imposed on the electrical gas heater elements in the loop.

RESULTS AND DISCUSSION

The purpose of this hot test was to verify the integrity of the complete BRU package and electrical controls at design turbine and compressor inlet temperatures and speed, and with loads on the alternator up to 6 kW.

System three phase electrical load unbalance, VR and speed control operating, and alternator operating temperatures will be discussed for various steady state power levels reached during this test.

Load Unbalance

Speed control was maintained within the design specification of .1 percent at each load level. The parasitic load power, however, showed large differences among the three phases. Table III presents the various electrical parameters as measured at the three system power levels covered during the tests. At each of these three levels as well as at all other times when the speed control was operating, load unbalance was observed. The ratios of phase power were not constant for changes in the frequency of the alternator output.

The primary cause of the load unbalance is the developing of unequal output voltages across the parasitic load resistor (at any frequency above 1200 Hz) for each of the output circuits in speed control unit 1. Variations in firing characteristics between SCR's and in the values of related network components are responsible.

The degree of load unbalance caused by operation of the second and third units of the speed control could not be determined during these test runs. With the second unit providing approximately 25 percent of its capacity at the 6 kW level the phase load balance improved.

The unbalance loads contributed to current flow in the neutral conductor. Since the unbalance was greatest at lower loads, the neutral currents were greater at these loads. At the 4.3 kW load point, the neutral current was 13.8 amperes. This current dropped to 11.5 amperes at the 6 kW load point.

Load Fluctuations

Electrical load fluctuations were observed at alternator outputs of 0.3 kW and at 4.6 kW. At these points the total load varied ± 0.15 kW with periods ranging from 0.5 to 3 seconds. Above 0.45 kW and below 0.3 kW the load was stable as it was above 4.6 kW and below 4.4 kW. These changes in load did not produce changes in machine speed.

The load fluctuations were not caused by interaction between the VR and the speed control. This was verified by using a d.c. power supply to excite the alternator fields. The fluctuations were again observed at the same total power and frequency values.

Each speed control unit is rated at 2 kW per phase, the total maximum loading capability for the three units being 18 kW. The first instability occurs when unit number one begins to apply load. The second occurs when unit number 2 begins to apply any additional required load. As was stated earlier, there is some overlap in the range of frequency response of each controller. This explains why the initial application of load by unit number 2 could occur at the 4.4 kW level.

The small conduction angles occurring during the operation of the first or second units at these loads would appear to relate to the fluctuation. During this period the exact SCR firing points seem unable to be fixed with consistency by the controllers.

VR - Speed Control

During the operation of the loop, the VR controlled the alternator output voltage at 120 volts line to neutral ± 1 percent. Picture 1 of figure 9 shows VR shunt field voltage at the 6 kW load level. The frequency of the pair of voltage pulses was determined to be 1218 Hz. This is the control point of the speed control at 6 kW. It is expected that the frequency of these pulses would be three times line frequency or 3654 Hz. It is also noted that the width of pulse 1 is greater than that of pulse 2.

Relating these observations to the discussion of the VR operation, data in table III and wave form photos shown in figure 10, the differences in peak values of phase voltage cause E_B to be less than E_R for different time intervals. Table III shows phase C line to neutral voltage to be the highest and its ripple peak thus produces nonuniformity in the ripple pattern. Since the B phase peak is also high, E_B never falls below E_R and the transistor never conducts at this point. This condition is the one shown graphically in figure 5. The nonuniform ripple also causes the lack of uniformity ($TC_1 > TC_2$) among the voltage pulses. Even if peak line voltage magnitudes were identical, distortions near the peaks could cause nonuniformity in the ripple pattern, thus producing similar effects.

This distortion in the line to neutral voltage wave is produced by the action of the speed control. Even when firing over the largest conduction angle (approx. 170°), some distortion is introduced. Passive network filters are used in these units and are designed to minimize radio frequency interference. They also provide a measure of reduction of harmonics in the alternator line voltage (figs. 10 and 11). This distortion increases as conduction angles are reduced because of less parasitic load being needed or when the second and third units are fractionally used. Distortion is maximized when any one unit is operating at a 90° SCR conduction angle.

If conduction angles are unequal for different phases of the same control unit, each phase voltage will have a different wave shape. From photographs of voltage across the parasitic load resistor (fig. 11), it is seen that conduction angles did indeed vary from phase to phase.

Waveform photos of shunt current output (fig. 9) display the rise and decay with the inductive load of the field circuit. Current flow is sustained through a diode across the shunt field winding during the time interval between VR output voltage pulses. Different peak

values of series field voltage (fig. 12) are partly the result of the line current distortion. Figure 13 shows this dissimilar distortion for each line current resulting from having different firing angles for each phase of the speed control units in operation.

When the load was reduced to 4.3 kW, the electrical system was affected in several ways. The VR shunt output voltage became a series of pulses with a frequency of 1215 Hz (fig. 14). The current waveform reflected this change and had the similar rise and decay pattern as observed previously. A line frequency of 1215 Hz corresponded to the speed control point at the 4.3 kW load level. Relating figure 14 to table I (fig. 15) and the VR operation outlined previously, E_B must now be less than E_R at only one point during the half wave three phase ripple cycle. This initiates switch action at the rate of one-third of the ripple frequency.

The series field voltage and current (fig. 16) repeat the patterns seen at the 6 kW condition. The series field voltage waveform is altered because of increased line current distortion and unbalance.

Figure 17 shows photographs of the output voltages of speed control unit 1 at the 4.3 kW level. The distortion level has increased particularly in the phase A and B outputs for this lower power level.

Alternator Temperatures

The alternator was designed for a constant cooling oil flow of 0.12 lb/sec (0.05 kg/sec). Thermal maps were calculated by the contractor for the 6 kW load level using this flow rate. Figure 18 shows the thermocouple locations on the alternator. Table IV gives a comparison of the calculated temperatures and the actual temperatures found under test using a flow rate of 0.146 lb/sec (0.066 kg/sec). This data shows that the armature windings are somewhat higher in temperature than calculated. The contractor stated that thermocouple numbers 1 and 3, and 2 and 4 might be reversed. If this is correct then the maximum difference between the calculated and actual temperatures is about 111° F (62 K) while the average winding temperature is 36° higher than the calculated average for thermocouple locations 1, 2, 3, 4, 9, and 10. At the 6 kW power level the maximum winding temperature was 371° F (462 K). This value is within the continuous operating rating of 430° F (494 K) for the armature windings. Table V gives alternator temperatures for three steady state power levels using a cooling flow rate of 0.146 lb/sec (0.066 kg/sec).

SUMMARY OF RESULTS

The results of the preliminary testing of the BRU alternator, VR, and speed control are summarized as follows:

1. Speed was controlled within the design specification of ± 1 percent at each load level tested. The speed control, however, introduced some phase load unbalance.

2. Electrical load fluctuations were observed at load levels corresponding to the frequency at which each speed control unit began to apply load. The load fluctuations, however, were small and did not result in any speed fluctuations.

3. The mode of operation of the shunt field regulator was affected by line voltage distortions produced by the speed controllers. This did not impair its proper functioning in the system, and voltage was controlled within ± 1 percent.

4. The measured armature winding temperatures were somewhat higher than the calculated values.

REFERENCES

1. Klann, John L.: 2 to 10 Kilowatt Solar or Radioisotope Brayton Power System. Intersociety Energy Conversion Engineering Conference. Vol. 1. IEEE, 1968, pp. 407-415.
2. Wong, Robert Y.; Klassen, Hugh A.; Evans, Robert C.; and Winzig, Charles H.: Experimental Investigation of a Single-Shaft Brayton Rotating Unit Designed for a 2- to 10-Kilowatt Space Power Generation System. NASA TM X-1869, 1969.
3. Repas, David S.; and Edkin, Richard A.: Performance Characteristics of a 14.3-Kilovolt-Ampere Modified Lundell Alternator for 1200 Hertz Brayton-Cycle Space-Power System. NASA TN D-5405, 1969.
4. Anon.: Design and Fabrication of the Brayton Cycle High Performance Compressor Research Package. Rept. No. APS-5269-R, AiResearch Mfg. Co. (NASA CR-72533), 1967.
5. Ingle, B. D.; and Corcoran, C. S.: Development of a 1200-Hertz Alternator and Controls for Space Power Systems. Intersociety Energy Conversion Engineering Conference. Vol. 1. IEEE, 1968, pp. 438-447.

TABLE I. - TURBINE-COMPRESSOR AND GAS BEARING DESIGN
 OPERATING CONDITIONS AT 10.7 kW ELECTRICAL LOAD

Turbine and Compressor	
Working fluid	HeXe Mixture - M = 83.8
Mass flow rate, lb/sec (kg/sec)	1.28 (0.5806)
Turbine inlet temperature, °R (K)	2060 (1144)
Turbine inlet pressure, psia (N/cm ² abs)	42.1 (290)
Compressor inlet temperature, °R (K)	540 (300)
Compressor inlet pressure, psia (N/cm ² abs)	22.9 (15.8)
Speed, rpm	36 000
Gas Bearings	
Working fluid	He-Xe Mixture
Ambient temperature, °R (K)	880 (489)
Ambient pressure, psia (N/cm ² abs)	42.0 (28.95)

TABLE II. - ELECTRICAL COMPONENT DESIGN SPECIFICATIONS

Alternator	
Output power, kW	10.7
Phase	3
Power factor	0.75
Voltage, V	120/208
Frequency, Hz	1200
Liquid coolant	Dow Corning 200
Liquid coolant inlet temperature, °R (K)	530 (294)
Liquid coolant flow rate, lb/sec (kg/sec)	0.12 (0.054)
Winding insulation temperature rating, °R (K)	887 (493)
Voltage regulator exciter	
Regulation (for balanced loads at rated power factor and frequency)	120 V ±1 percent
Response time (within ±5 percent of steady state voltage)	1/4 second
Voltage regulator internal loss (at 120 V line to neutral and 1 per unit alternating line current)	41 watts
Speed Control	
Speed regulation (for a change in load from 10 percent to full load)	±1 percent
Response time (within ±2 percent of steady state speed)	1 second
Internal losses each unit (Minimum total parasitic load)	13 watts

TABLE III. - ELECTRICAL PARAMETERS AT VARIOUS
SYSTEM POWER LEVELS

Total parasitic load power, kW	4.3	5.0	6.0
Power factor	0.84	0.88	0.89
Line to neutral voltage, V			
Phase A	120.6	120.0	121.1
Phase B	125.1	123.9	123.4
Phase C	122.6	123.5	124.0
Line current, A			
Phase A	14.5	17.4	19.9
Phase B	10.1	12.1	16.5
Phase C	17.0	17.3	18.9
Neutral current, A	13.8	11.6	11.5
Parasitic load power, kW			
Phase A	1.5	2.0	2.3
Phase B	0.8	1.0	1.5
Phase C	2.0	2.0	2.2
Shunt field voltage, V	3.0	3.47	4.26
Shunt field current, A	1.20	1.27	1.40
Series field voltage, V	4.0	4.40	5.25
Series field current, A	1.40	1.43	1.67
Frequency, Hz	1215	1215	1218

TABLE IV. - COMPARISON OF CALCULATED AND ACTUAL ALTERNATOR

TEMPERATURES AT 6.0 kW

Thermocouple location	Calculated, ^a °F	Actual, °F	Thermocouple location	Calculated, ^a °F	Actual, °F
1	275	206	9	140	131
2	260	239	10	135	133
3	200	344	11	140	131
4	200	371	12	135	120
5	350	349	13	400	445
6	200	274	14	210	228
7	200	273	15	230	232
8	200	276			

^aP.F. - 0.85.

TABLE V. - ALTERNATOR TEMPERATURES FOR THREE STEADY
STATE POWER LEVELS - COOLING FLOW RATE 0.146 lb/sec

Thermocouple number	4.30 kW, °F	5.02 kW, °F	6.08 kW, °F
1	170	183	206
2	189	207	239
3	266	293	344
4	279	313	371
5	269	298	349
6	217	238	274
7	216	236	273
8	218	239	276
9	116	121	131
10	115	121	133
11	122	125	131
12	107	110	120
13	335	372	445
14	175	197	228
15	196	208	232

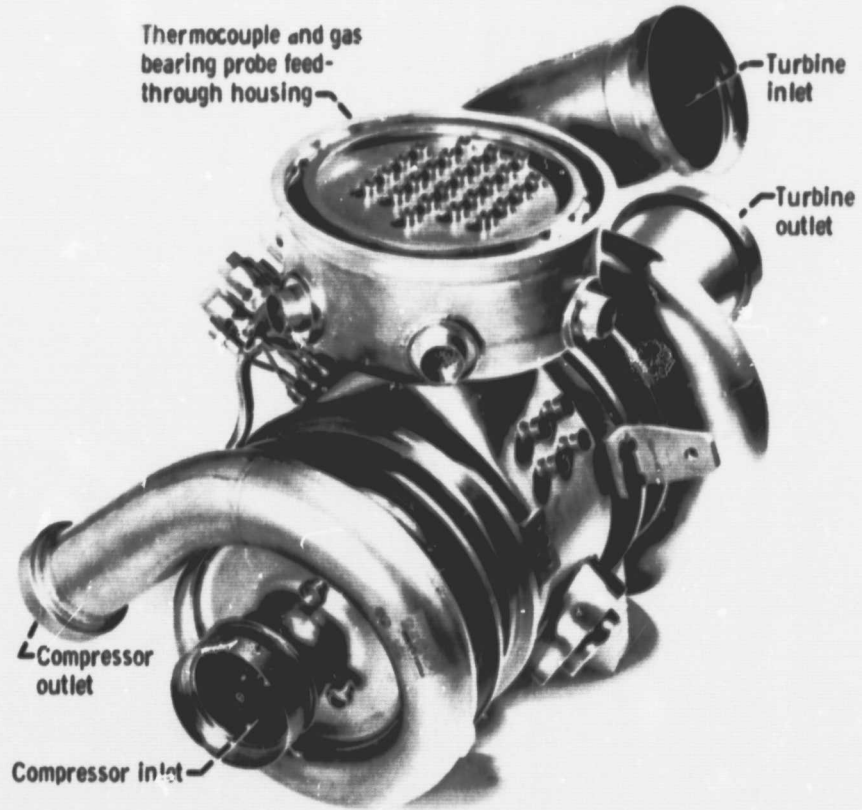


Figure 1. - Brayton rotating unit.

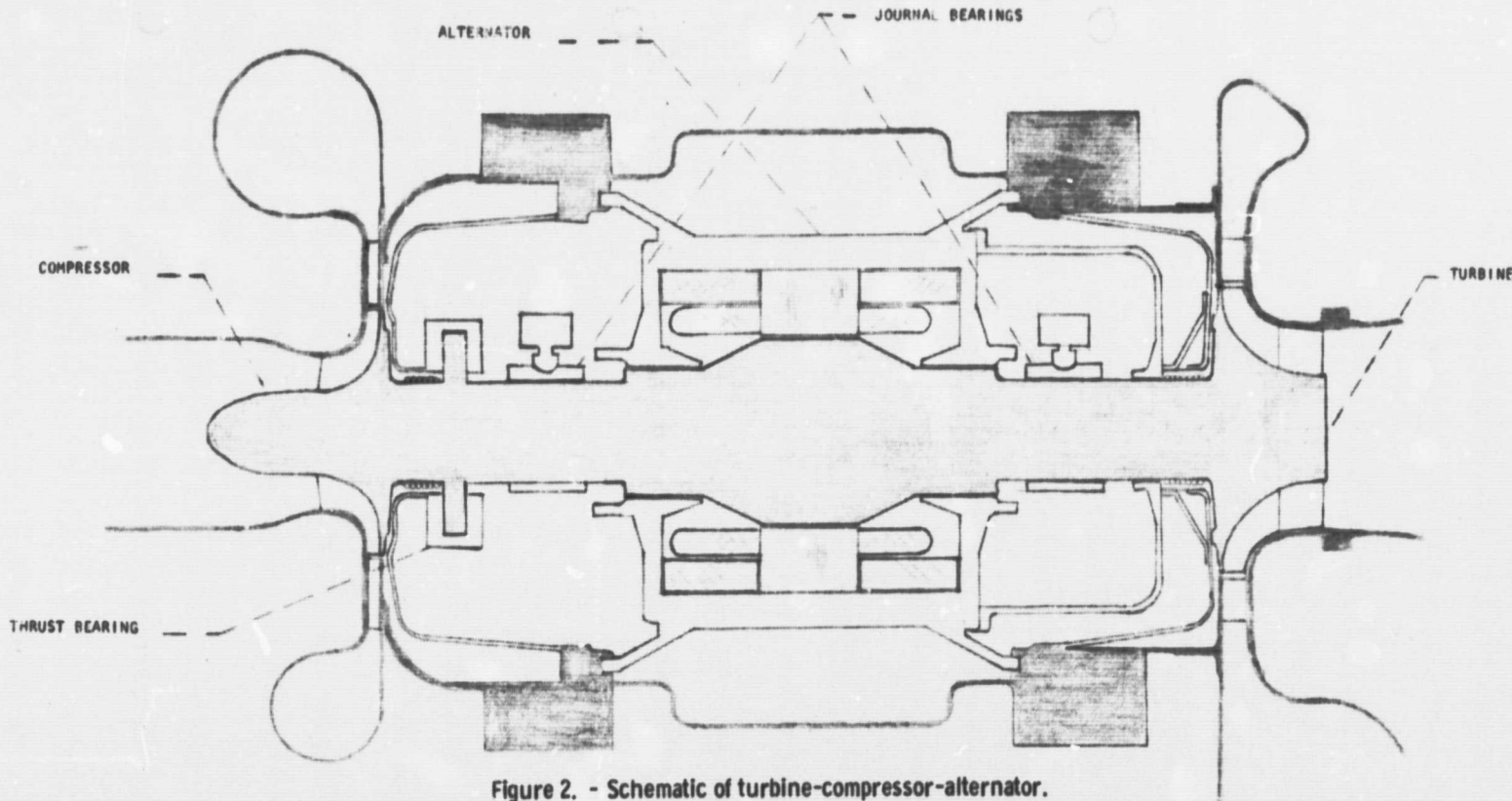


Figure 2. - Schematic of turbine-compressor-alternator.

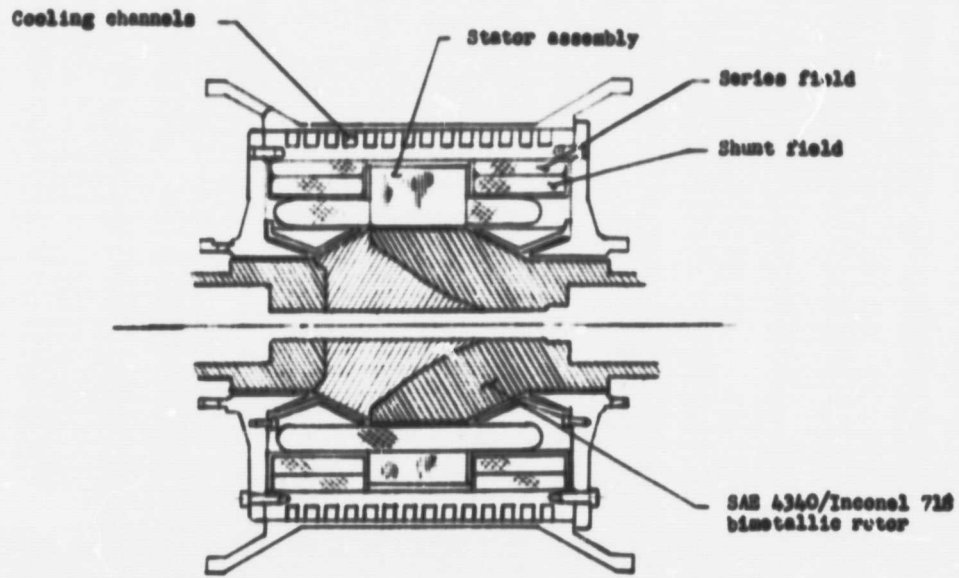


Figure 3. - Sectional view of BRU alternator.

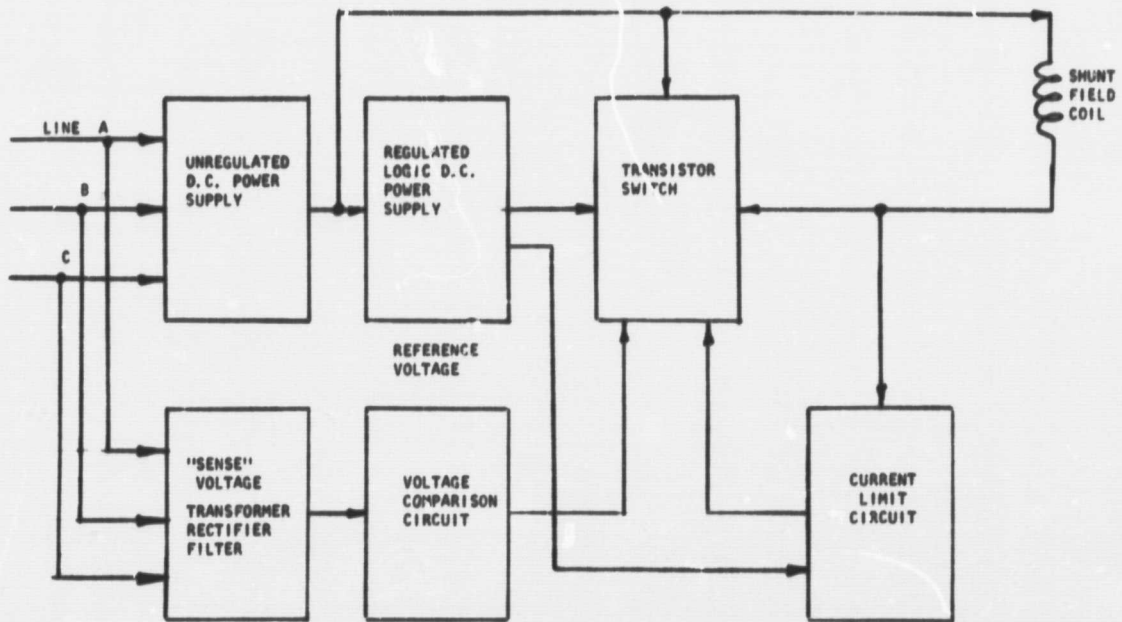
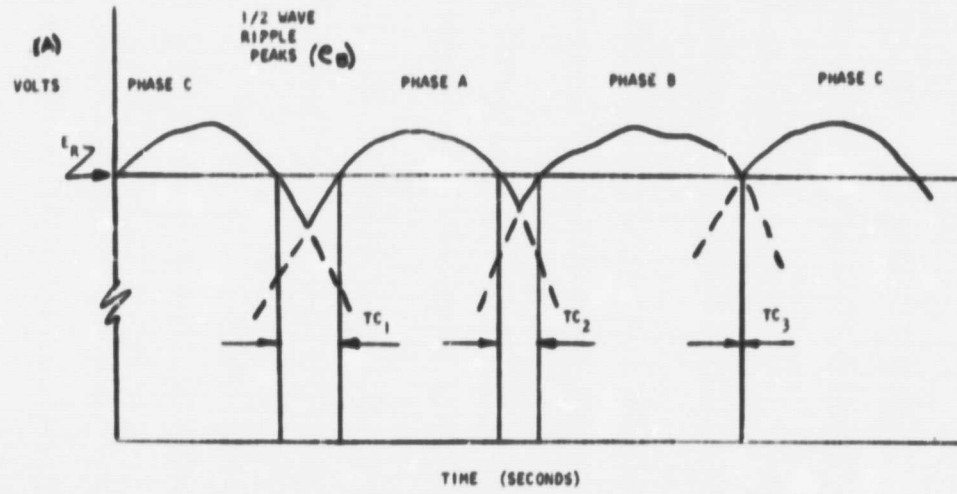
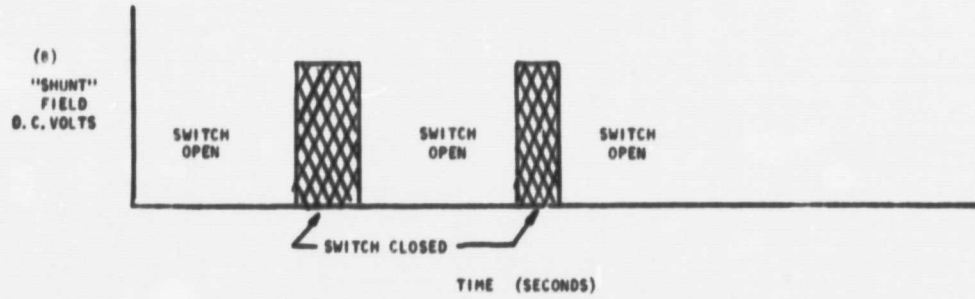


Figure 4. - Block diagram of shunt field regulator (VR).



(a) Comparison crt. wave forms.



(b) Shunt regulator switch action.

Figure 5. - VRE.

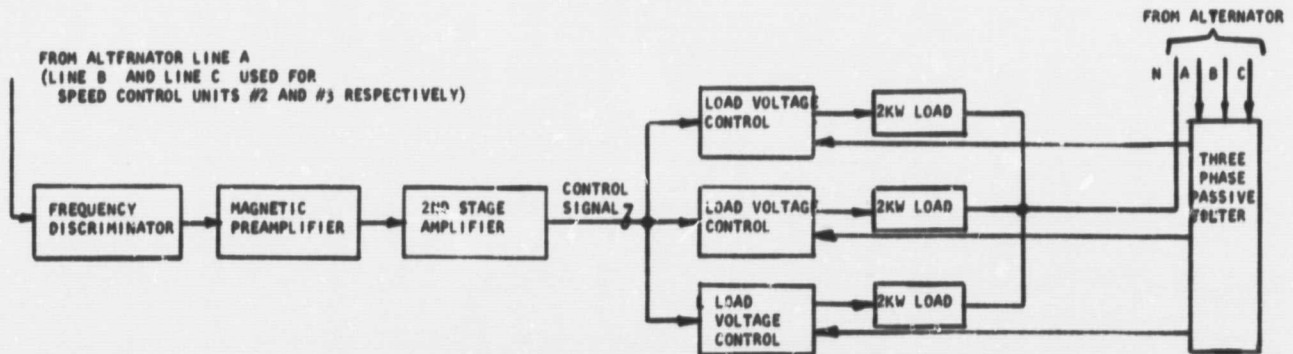


Figure 6. - Block diagram of speed control #1 (units #2 and #3 identical).

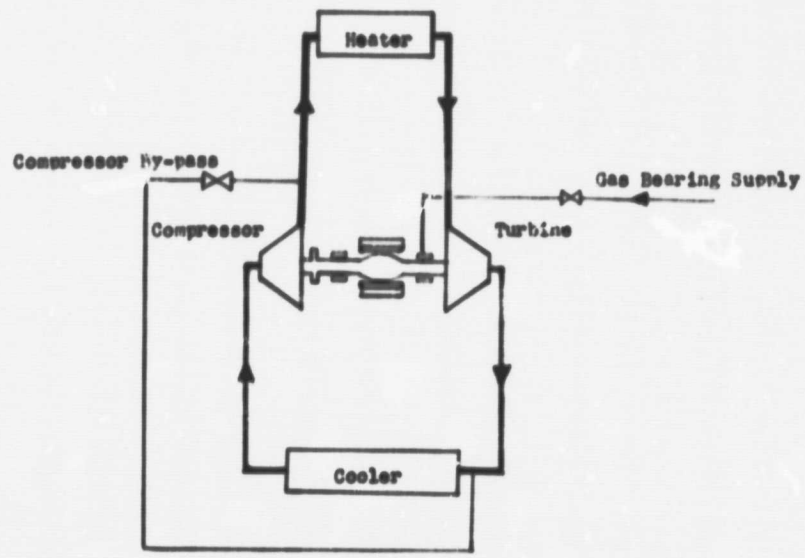


Figure 7. - Schematic diagram of test loop.

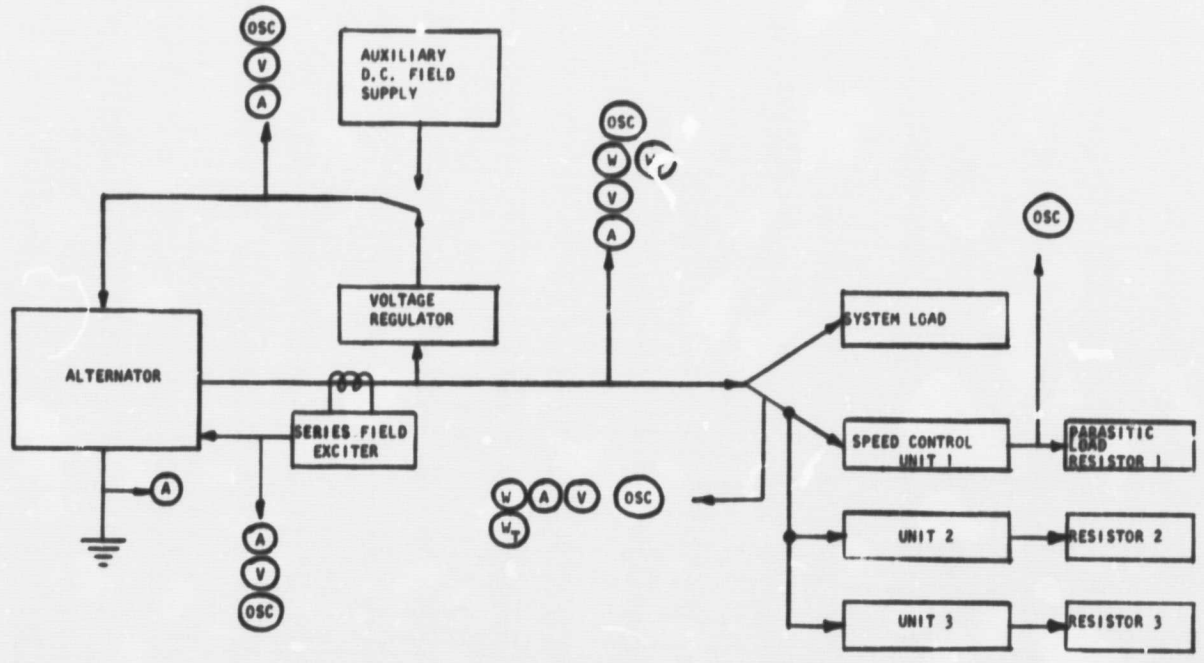


Figure 8. - Block diagram of electrical system.

E-5214

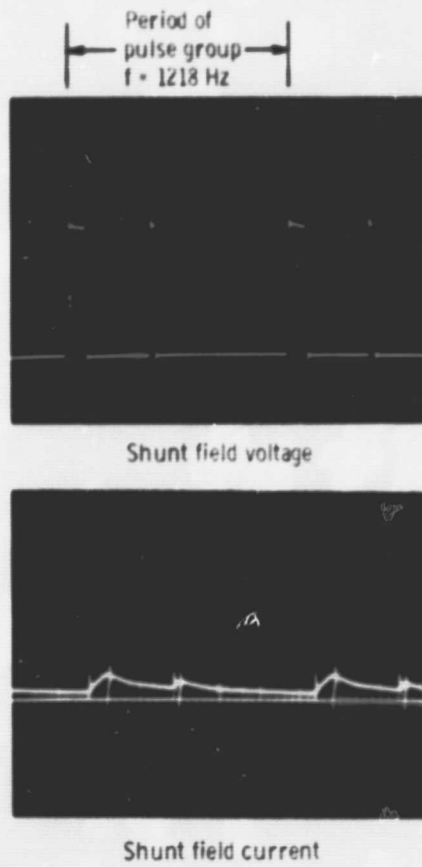


Figure 9. - VRE shunt field voltage and current at 6.0 kW load.

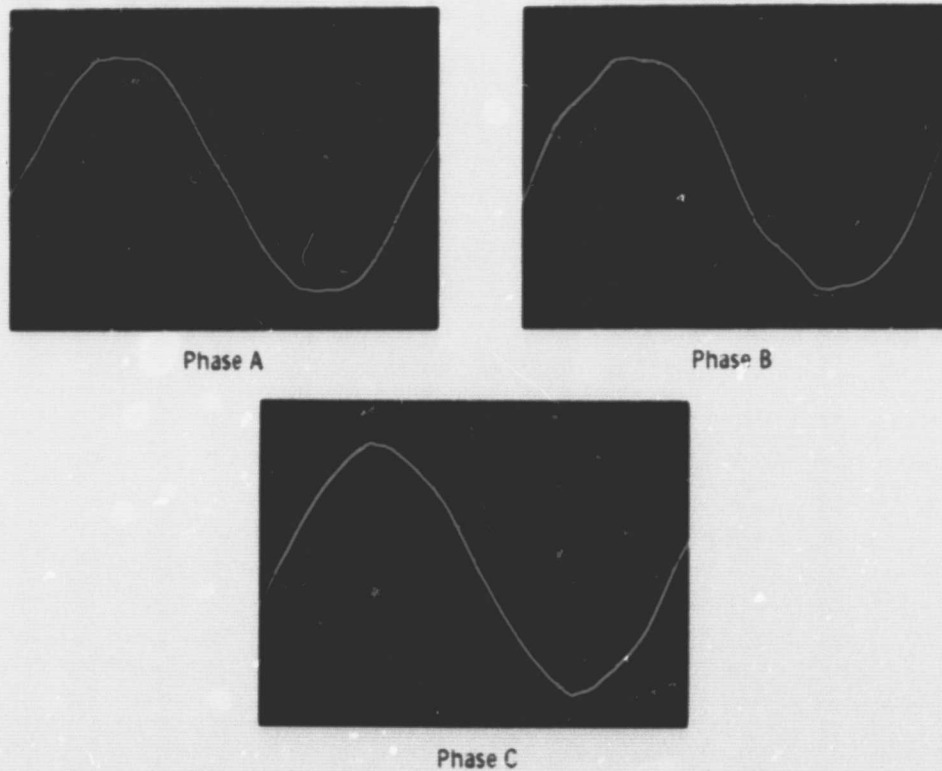


Figure 10. - Alternator line to neutral voltage at 6.0 kW load.

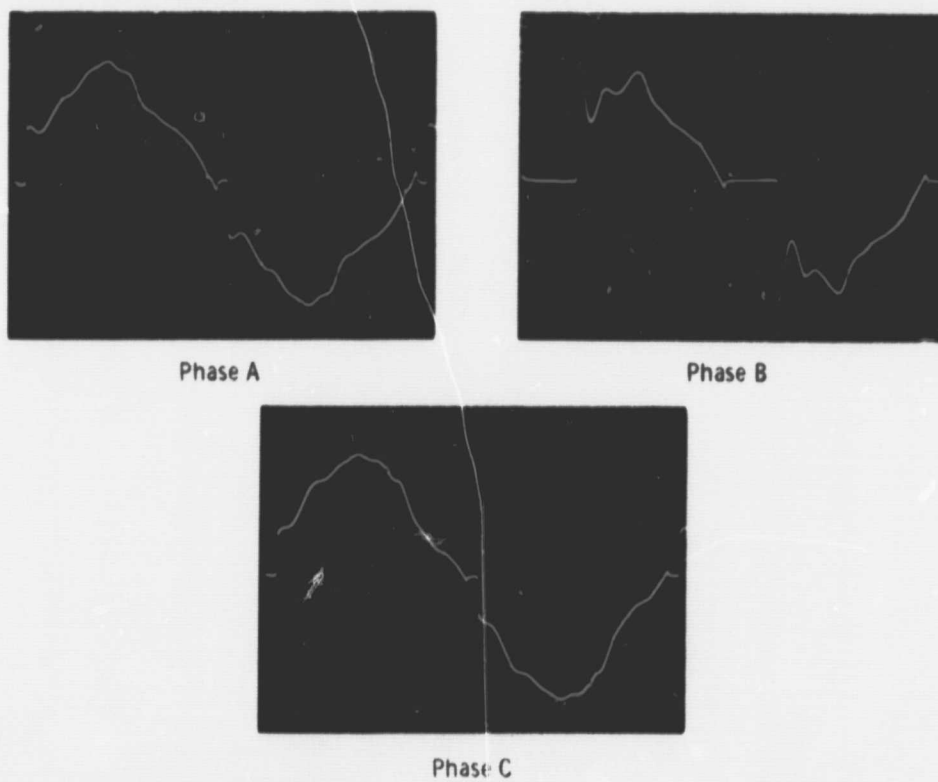


Figure 11. - Speed control unit #1 output line to neutral voltage at 6.0 kW load.

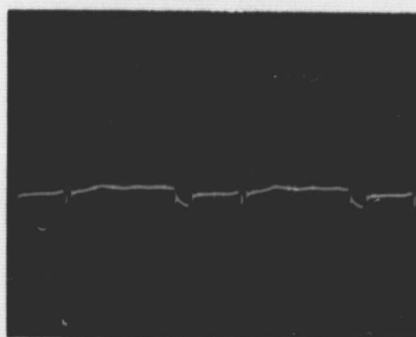
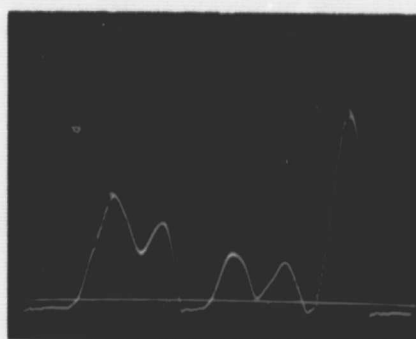


Figure 12. - VRE series field voltage and current at 6.0 kW load.

E-5214

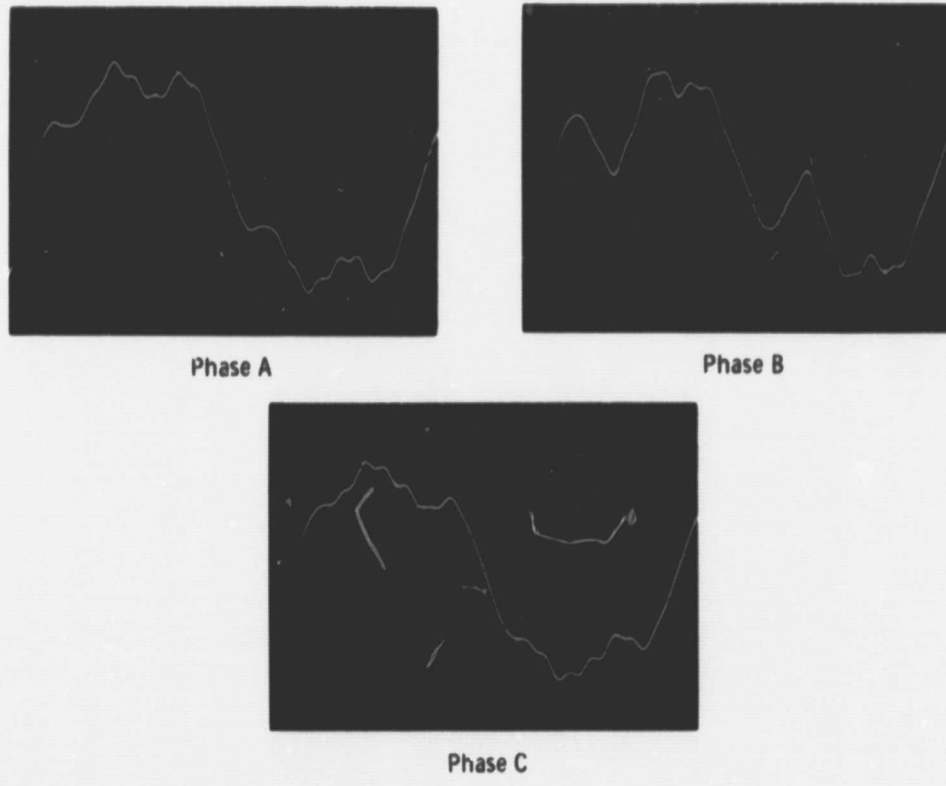


Figure 13. - Alternator line current at 6.0 kW load.

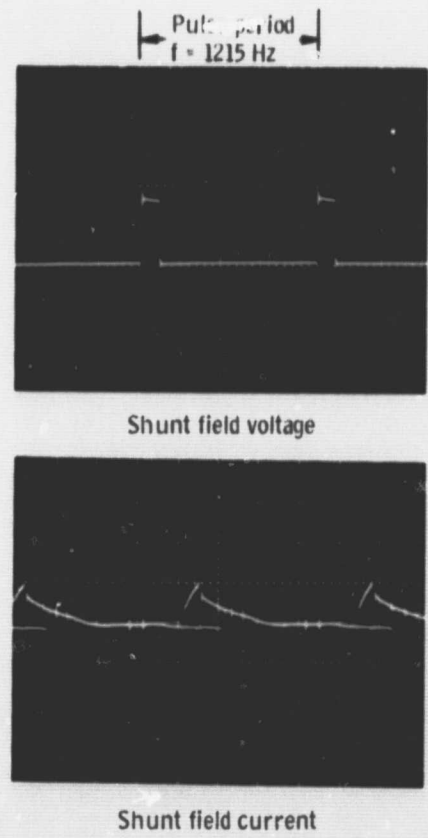


Figure 14. - VRE shunt field voltage and current at 4.3 kW load.

E-5214

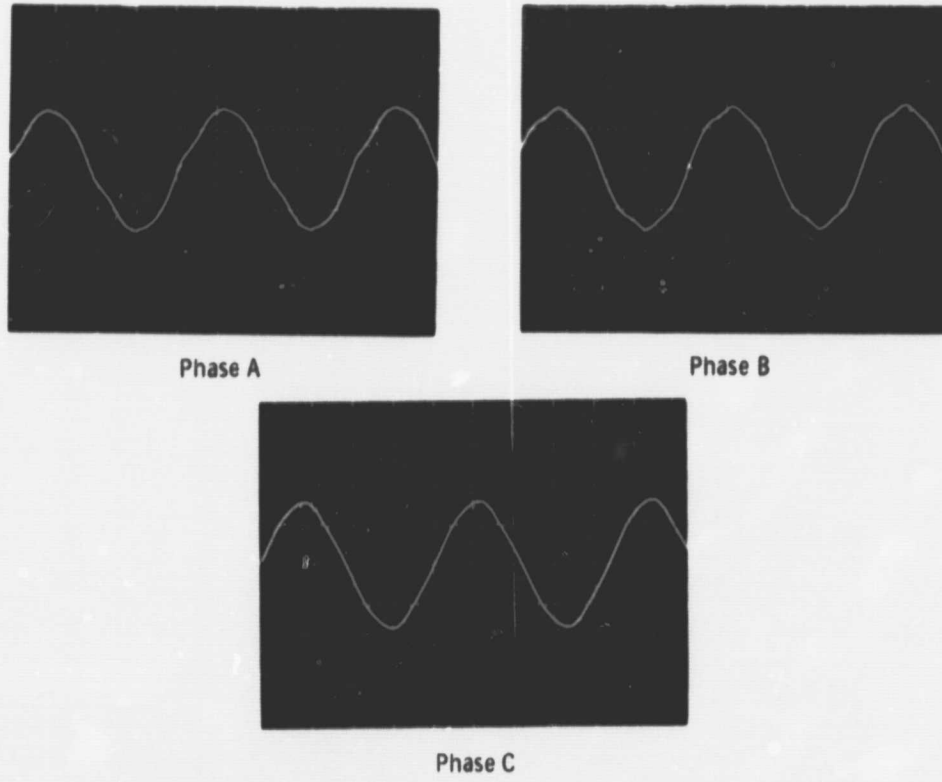


Figure 15. - Alternator line to neutral voltage 4.3 kW load.

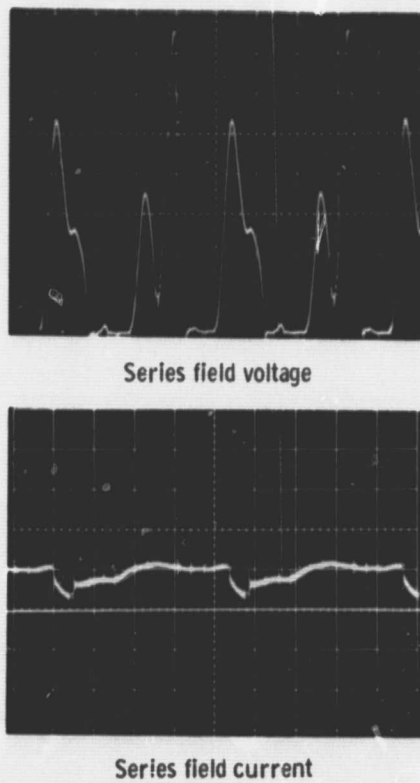


Figure 16. - VRE series field voltage and current at 4.3 kW load.

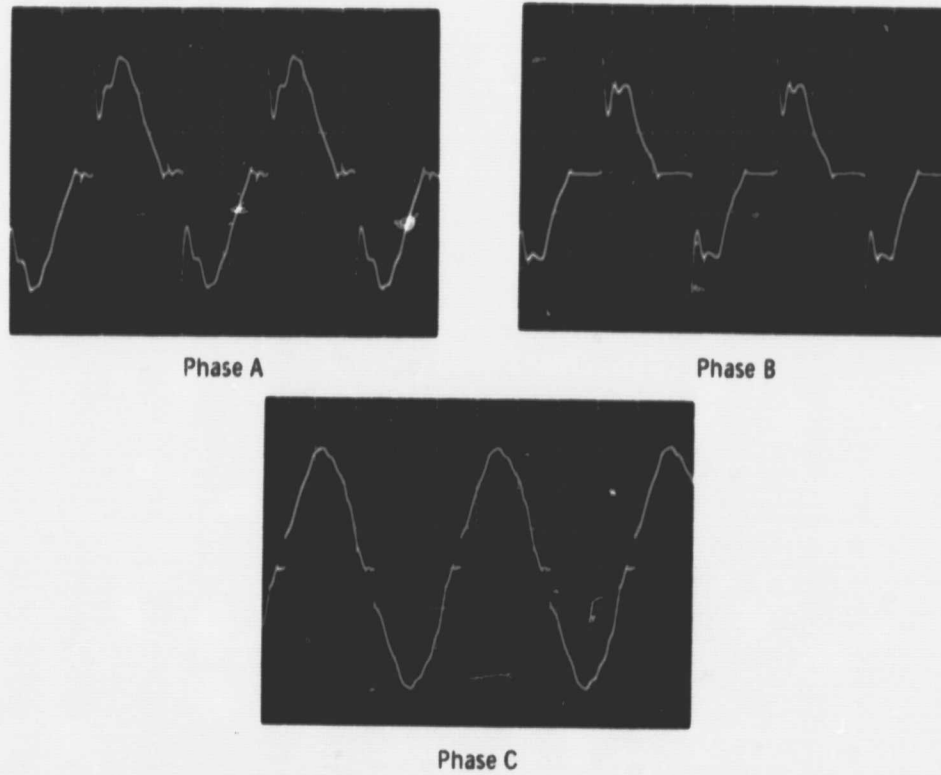


Figure 17. - Speed control unit #1 output line to neutral voltage 4.3 kW load.

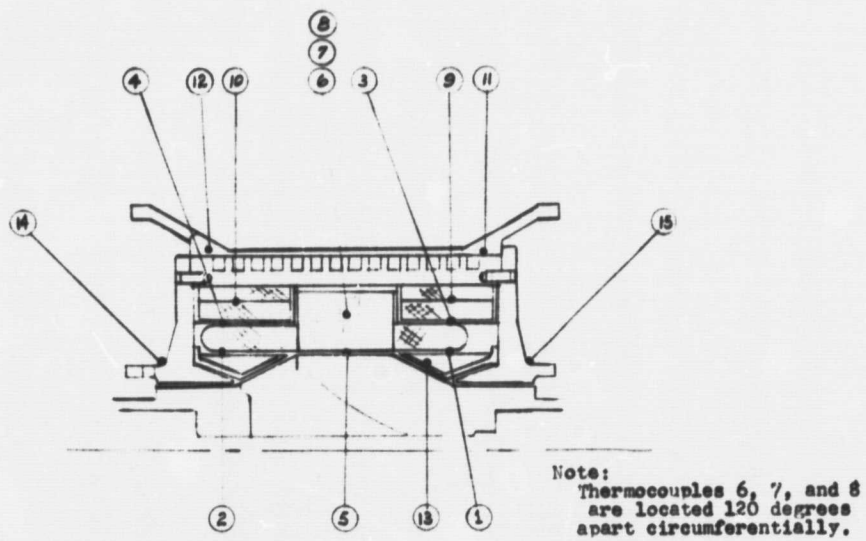


Figure 18. - Alternator thermocouple locations.